Proc. Natl. Acad. Sci. USA
Vol. 93, pp. 8413–8418, August 1996
Cell Biology

Toxoplasma invasion: The parasitophorous vacuole is formed from host cell plasma membrane and pinches off via a fission pore

(cell capacitance/intracellular parasite/endocytosis)

E. SUSS-TOBY*, J. ZIMMERBERG*†, AND G. E. WARD‡

*Laboratory of Theoretical and Physical Biology, National Institute of Child Health and Human Development, and ‡Laboratory of Parasitic Diseases, National Institute of Allergy and Infectious Diseases, National Institutes of Health, Bethesda, MD 20892

Communicated by Louis H. Miller, National Institutes of Health, Bethesda, MD, May 1, 1996 (received for review March 10, 1996)

ABSTRACT **Most intracellular pathogens avoid lysing their host cells during invasion by wrapping themselves in a vacuolar membrane. This parasitophorous vacuole membrane (PVM) is often retained, serving as a critical transport interface between the parasite and the host cell cytoplasm. To test whether the PVM formed by the parasite *Toxoplasma gondii* is derived from host cell membrane or from lipids secreted by the parasite, we used time-resolved capacitance measurements and video microscopy to assay host cell surface area during invasion. We observed no significant change in host cell surface area during PVM formation, demonstrating that the PVM consists primarily of invaginated host cell membrane. Pinching off of the PVM from the host cell membrane occurred after an unexpected delay (34–305 sec) and was seen as a 0.219 ± 0.006 pF drop in capacitance, which corresponds well to the predicted surface area of the entire PVM (30–33 μm^2). The formation and closure of a fission pore connecting the extracellular medium and the vacuolar space was detected as the PVM pinched off. This final stage of parasite entry was accomplished without any breach in cell membrane integrity.**

Toxoplasma gondii is an important pathogen of humans, causing congenital birth defects when acute infection occurs during pregnancy, and severe encephalitis in immunocompromised persons. Toxoplasmic encephalitis has recently emerged as one of the most serious opportunistic infections associated with AIDS (1, 2). Like other Apicomplexan parasites (including *Plasmodium*, the causative agent of malaria), *T. gondii* is an obligate intracellular parasite. During invasion, which is an active process distinctly different from phagocytosis (3), the parasite becomes surrounded by the PVM. The PVM pinches off from the host cell membrane at the end of invasion, to create a vacuole within which the parasite grows and replicates to continue the infection. As the interface between the parasite and the host cell, the PVM functions in metabolite uptake, nutrient transport, and protein trafficking (4–7).

The origin of the PVM in cells infected with *Toxoplasma* and other Apicomplexan parasites is unknown, and has been the subject of considerable controversy (8–11). Two main models have been proposed to explain how the PVM is formed. In the bilayer insertion model, the PVM is thought to be formed from lipids that are secreted from apical organelles of the parasite and inserted into the host cell membrane during invasion. Evidence supporting this model includes the absence of host cell membrane proteins from the forming PVM (12–15), and the presence of membrane-like lamellar structures within and emanating from the parasite's apical secretory organelles (16–18). An alternative model, induced invagination, proposes that the parasite induces the host cell membrane to invaginate to form the PVM. Evidence supporting this model includes the similar lipid compositions of the host cell membrane and the developing PVM (8). As discussed elsewhere (8, 9), neither model can be rejected on the basis of the data thus far reported.

The bilayer insertion model predicts a significant increase in surface area during PVM formation, followed by a drop in surface area as the PVM pinches off. The induced invagination model predicts no significant increase in surface area during PVM formation, followed by a drop in surface area as the PVM pinches off. We report here experiments designed to directly test these predictions, using time-resolved capacitance measurements to measure host cell surface area (19) while simultaneously monitoring invasion optically (20).

MATERIALS AND METHODS

Host Cells and Parasites. COS-1 cells (ATCC CRL 1650) were cultured in complete Dulbecco's modified Eagle's medium (DMEM) at 37°C, released from the culture dishes by trypsinization (2 min in 0.25% trypsin, 1 mM EDTA) and allowed to settle onto a 35 mm ΔT dish (Bioptechs, Butler, PA) in complete DMEM for 30–90 min at 37°C prior to use. *T. gondii* (RH strain) tachyzoites were cultured in human foreskin fibroblasts (ATCC CRL 1634) as described (3). Spontaneously released parasites from a massively infected monolayer (multiplicity of infection ≥10) were passed twice through a 27G needle, filtered through a 10-μm PCTE filter (Poretics, Livermore, CA), spun for 5 min at 1100 × *g*, and resuspended in bath solution (see below).

Optical Visualization of Invasion. Experiments were performed in bath solution at 35°C, using a Focht stage heating system (Bioptechs) on a Zeiss IM35 inverted microscope equipped with differential interference contrast (DIC) and epifluorescence optics. The parasite suspension was loaded into a beveled parasite delivery pipette (15-μm opening), and delivered to the COS-1 cells using an Eppendorf 5242 microinjector. Microscope images were collected using a Dage–MTI (Michigan City, IN) VE1000 SIT video camera, recorded on a Sony BVU-950 videocassette recorder, digitized using a PCVISIONplus capture board, and processed postcapture using Image-Pro Plus (Media Cybernetics, Silver Spring, MD).

For the fluorescence invasion assay, anti-P30 monoclonal antibody (Biogenex Laboratories, San Ramon, CA) was conjugated with fluorescein as follows. Sodium bicarbonate (200 μl, 1M) and 6-(fluorescein-5-(and-6)-carboxamido) hexanoic acid, succinimidyl ester (100 μl, 10 mg/ml) were added sequentially to 1 ml (250 mg) of anti-P30, and incubated for 90 min at 23°C. The reaction was stopped with hydroxylamine (100 μl, 1.5 M, pH 8.0), incubated 30 min at 23°C, and passed through a PD-10 column (Pharmacia) equilibrated with phosphate buffered saline (PBS). The excluded fraction containing the conjugate (1.4 ml) was collected, sterile filtered, and stored

The publication costs of this article were defrayed in part by page charge payment. This article must therefore be hereby marked "*advertisement*" in accordance with 18 U.S.C. §1734 solely to indicate this fact.

Abbreviations: PVM, parasitophorous vacuole membrane; EOC, end of constriction; DIC, differential interference contrast.

†To whom reprint requests should be addressed.

at 4°C. To assay invasion using the conjugate, the microscope stage heater was turned off, and the bath solution was replaced with chilled (4°C) PBS containing 0.5% (wt/vol) bovine serum albumin (PBS/BSA). After 4 min, this solution was replaced with 1.5 ml PBS/BSA containing 30 μl fluorescein-conjugated anti-P30, and incubated for 12 min at 23°C. The dish was washed four times with chilled PBS/BSA (3 ml each for 3 min) and viewed with epifluorescence optics.

Electrophysiology. The bath solution contained: 118 mM NaCl/5.85 mM KCl/1.2 mM $MgCl_2$/2.52 mM $CaCl_2$/11 mM glucose/5 mM Hepes (pH 7.4) with NaOH (21). The pipette solution for whole-cell recordings contained either 122 mM KCl, or 102 mM Kaspartate and 18 mM KCl, in addition to 2 mM $MgCl_2$/11 mM EGTA/1 mM $CaCl_2$/5 mM Hepes/1 mM ATP/0.5 mM GTP (pH 7.26) with KOH. The pipette solution for the perforated patch contained 240 μg/ml amphotericin B in 130 mM methanesulfonate/10 mM KCl/8 mM $MgCl_2$/10 mM Hepes (pH 7.3) with KOH. Patch pipettes (1.5 MOhm resistance) were prepared from TW150-4 glass (World Precision Instruments, Sarasota, FL).

The imaginary and real parts of the cell admittance were calculated from the output current of an EPC7 patch clamp amplifier (List Electronics, Darmstadt, Germany) in the voltage clamp mode, using a digital lock-in amplifier (software available upon request). A 1000 Hz 80 mV peak-to-peak sine wave superimposed on a −12 mV holding potential was applied using an Axolab computer interface (Axon Instruments, Foster City, CA). The output current was filtered with a Butterworth low pass filter (Frequency Devices, Haverhill, MA) at a corner frequency of 5 kHz and digitized every 32 μS. The lock-in outputs represent the changes in capacitance (ΔC) and AC conductance (ΔG_{ac}) of the capacitor of a vacuole (C_v) in series with the conductance of a fission pore (G_p), as given by (20): $\Delta G_{ac} = [(\omega C_v)^2/G_p]/[1 + (\omega C_v/G_p)^2]$ and $\Delta C = (\omega C_v)/[(1 + (\omega C_v/G_p)^2]$ where $\omega = Z\pi f$ and f is frequency of applied sine wave). G_p was calculated from these equations as well as from the combined expression $G_p = [(\Delta G_{ac})^2 + (\Delta C^2)]/\Delta G_{ac}$.

RESULTS

Experiments were performed as shown in Fig. 1*a*, using the patch clamp technique in the whole cell (22) or perforated patch (23) configuration. The cell capacitance and conductance were calculated and inserted in real-time into the lower left-hand corner of the image from the microscope, allowing both optical and electrical measurements to be recorded on each video frame (20).

Parasites glide along the coverslip and surface of the cell at approximately 1 μm/sec with a characteristic twisting motion. The gliding stops immediately prior to invasion, when the apical end of the parasite attaches to the host cell plasma membrane (Fig. 1*b*, 0 sec). Interestingly, when the apical end of the parasite first attaches to the host cell, a large transient in host cell membrane conductance (spike) is invariably observed ($n > 100$; see star in Fig. 1*a*, G_{ac}). The nature and significance of the spike is currently under investigation; we used the time of the spike in this study to define the zero time of invasion. A constriction, readily visible with DIC optics, then develops at the apical end of the parasite and passes along the length of the parasite as it squeezes into the developing PVM (Fig. 1*b*, 19 sec and 39 sec). This constriction is the hallmark of an invading parasite (3). To independently confirm that a constricting parasite had indeed internalized, we developed an immunofluorescence assay in which free parasites and parasites bound to the external surface of the cell were brightly fluorescent, while internalized parasites were inaccessible to the antibody and were not stained (Fig. 1*b*, DIC and α-P30).

The capacitance of the host cell did not increase during PVM formation (Fig. 2*a–c*). Two different methods were used to quantitate capacitance changes during PVM formation (as depicted in Fig. 2*d*, the PVM is formed during the period of parasite constriction). In the first method, we assumed that any lipid insertion by the parasite would occur at a linear rate, based on the constant rate at which the parasite penetrates into the host cell (G.E.W., unpublished data). This assumption allowed us to fit to our capacitance data a continuous regression curve consisting of two linear segments: one prior to the spike, and one during the period of PVM formation. The change in capacitance was calculated as the difference between the slopes of these two linear segments, multiplied by the constriction time. By this method, host cell capacitance changed an average of 0.000 ± 0.017 pF (SEM, $n = 11$). In the second method of analysis, we made no assumptions about the rate of potential lipid insertion. The average capacitance during a 2-sec period immediately preceding the spike was subtracted from the average capacitance during the final 2 sec of parasite constriction. By this method, host cell capacitance changed an average of 0.000 ± 0.023 pF (SEM; $n = 11$).

Since the capacitance change associated with pinching off of the PVM was found to be −0.219 pF (see below), these data are clearly inconsistent (Student's t test, $\alpha = 0.005$) with the hypothesis that the PVM is composed primarily of newly inserted bilayer, which would predict an increase in host cell capacitance during invasion of this magnitude. The mean change we measured by both methods of analysis was zero, and the data allow us to rule out ($\alpha = 0.05$) any hypothesis in which there is a change of greater than 0.031 pF (method 1) or 0.041 pF (method 2), which corresponds to 14.2% or 18.5% of the total surface area of the PVM, respectively. Capacitance measures the net surface area, and while it is possible that the host cell tightly regulates its surface area and compensates for parasite-added lipids by taking up membrane as lipids are inserted, there was no evidence for such regulation after a substantial loss of membrane, the pinching off of the PVM (see below).

The expected drops in capacitance associated with pinching off of the PVM from the host cell membrane are clearly seen in Fig. 2*a–c* (asterisks). More than one third of the drops in capacitance ($n = 29$) fluctuated (e.g., Fig. 2*c*; see below). The average magnitude of the capacitance drop was 0.219 ± 0.006 pF (SEM, $n = 29$; Fig. 3*a*). When a cell was invaded by more than one parasite, multiple capacitance drops were seen, all of approximately the same magnitude (e.g., 0.22, 0.21, and 0.23 pF in Fig. 3*b*). If we model the parasite as two overlapping prolate ellipsoids with negligible separation of parasite and PVM (3), the calculated surface area of the PVM would be 30–33 μm^2. This yields a specific capacitance of the PVM of 0.0067–0.0073 $pF/\mu m^2$, within the range of biological membranes (20, 24, 25) and remarkably close to measurements of solvent-free planar bilayer membranes (26). Surprisingly, pinching off of the PVM did not occur at the end of constriction (EOC); the time between EOC and the drop was on average 201 ± 31 sec (SEM, $n = 6$) with an aspartate-based internal solution, 122 ± 16 sec ($n = 7$) with a chloride-based internal solution, and 73 ± 3 sec ($n = 4$) under perforated patch conditions.

Our measurement of the electrical parameters of the cell membrane during the entire process of invasion allowed us to detect the parasite-induced fission pore. A fission pore is the small aqueous connection between a forming endocytic vacuole (here, the parasitophorous vacuole) and the extracellular medium that forms and constricts to closure during the final stages of vacuole pinch off. A conceptually similar pore develops and widens during exocytosis, upon the formation of the first aqueous connection between the fusing exocytotic granule and the extracellular space (20, 27). As a fission pore closes, it creates impedence to the free diffusion of ions between the vacuolar space and the extracellular fluid, represented by a resistor in the equivalent circuit shown in Fig. 3*b* (*inset*). Analysis of our data based on this equivalent circuit

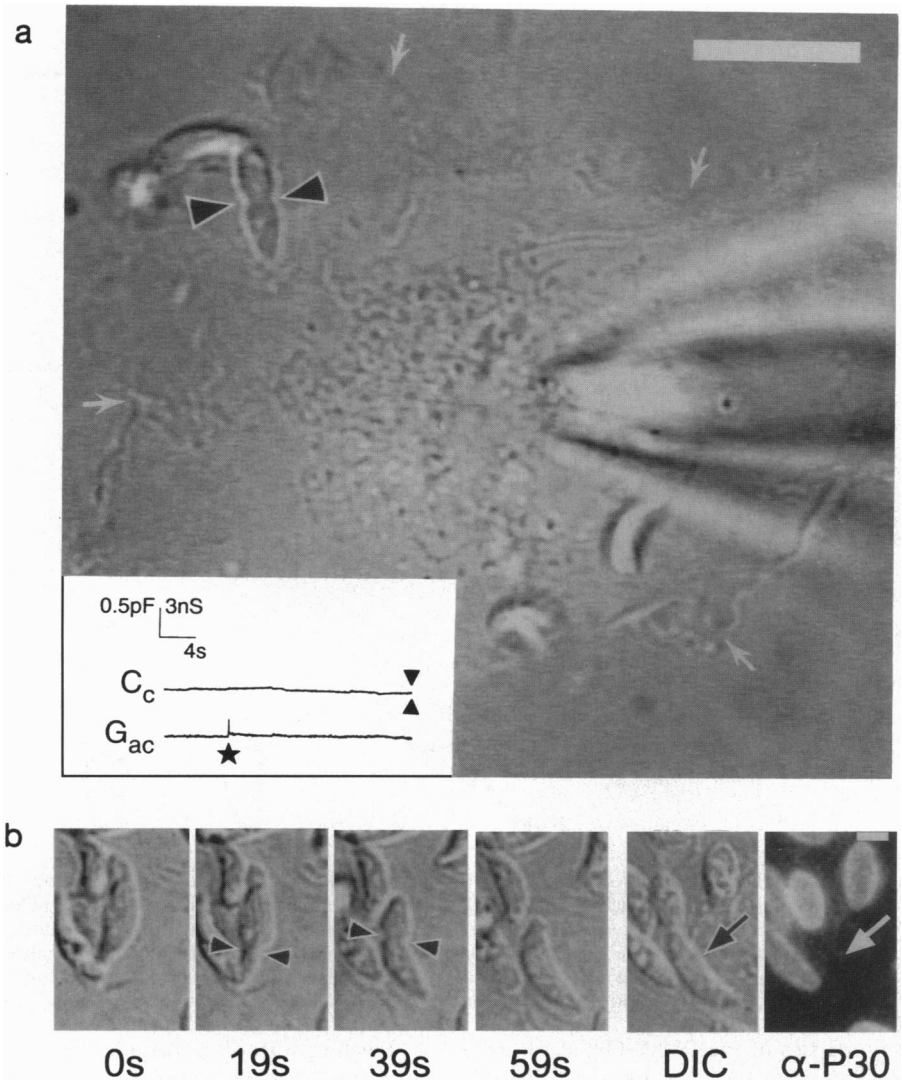

FIG. 1. (*a*) Simultaneous electrical and optical recording during the invasion of a partially spread COS-1 cell by *T. gondii* parasites. Parasites were delivered to the cell (edges of the cell are indicated by white arrows) using a micropipette (not shown); one parasite is in the process of invasion (black arrowheads). The patch pipette is seen on the right. A video image of the computer monitor displaying the real-time digital lock in amplifier calculations is inserted into the lower left hand corner of the microscope image using an RCA screen splitter. A graphical representation of the video insert is shown here, including the spike which precedes invasion (star, G_{ac} trace). c is the out-of-phase component of the measured admittance for the clamped cell and G_{ac} is the in-phase component of the admittance. Scale bar = 10 μm. (*b*) Visualization of parasite constriction during invasion, and inaccessibility of internalized parasites to an antibody against the parasite surface protein P30 (SAG1). Single video frames of DIC images captured during invasion, showing attachment (0 sec), and the constriction (19 sec and 39 sec; arrowheads), which passes along the length of the parasite, from anterior to posterior, as the parasite invades. In unclamped cells, the mean time from apical attachment to the EOC was 42.9 ± 11.8 sec (SEM, n = 10). In clamped cells, the mean "constriction time" from the spike until EOC was similar: 36.2 ± 8.75 sec (SEM, n = 48, whole cell conditions) and 38.5 ± 8.8 sec (SEM, n = 13, perforated patch). The microscope dish was subsequently incubated (15 min, 10°C) with fluorescein-conjugated anti-P30. After washing away unbound antibody, free parasites and parasites bound to the external surface of the cell were brightly fluorescent, whereas the internalized parasite (arrow) was inaccessible to the externally applied antibody and was not stained (DIC: image taken after processing for fluorescence; α-P30, fluorescence). (Bar = 2.5 μm.)

(see *Materials and Methods*) showed the dynamics of parasitic fission pore constriction (Fig. 3*c*). The fission pore conductance was at first too large to be measured, and then declined to an initial measurable value (Fig. 3*c*, G_p). As it closed further, the pore conductance frequently lingered at conductances with mean values that were momentarily stationary, indicating one or more semistable intermediate stages prior to complete closure. Detected pore conductances ranged from 12 to 0.1 nS, a range that, at its lower limit, overlaps with that of molecular ionic channels. The capacitance fluctuations described above reflected a rapid relaxation from a semistable pore conductance to a larger conductance, followed by a second (or third) constriction and complete closure (e.g., Fig. 3*c*). Fission pore conductances calculated from both C and G_{ac} were in accord with the fission pore conductances calculated from C alone (data not shown); no additional increase in cell conductance, which would indicate a breach in cell integrity, was detected.

DISCUSSION

This report represents the first application of electrophysiological methods to the study of host cell invasion during parasitic infection. The capacitance data show that while a small amount of parasite-derived material (0–18.5% of the total surface area of the PVM) may be inserted into the host cell membrane during invasion, most if not all of the PVM is derived from the host cell plasma membrane. Specific proteins (28, 29) and lipids (30) are thought to be transferred from the apical organelles of the parasite to the host cell during invasion, and might serve to induce the invagination or to

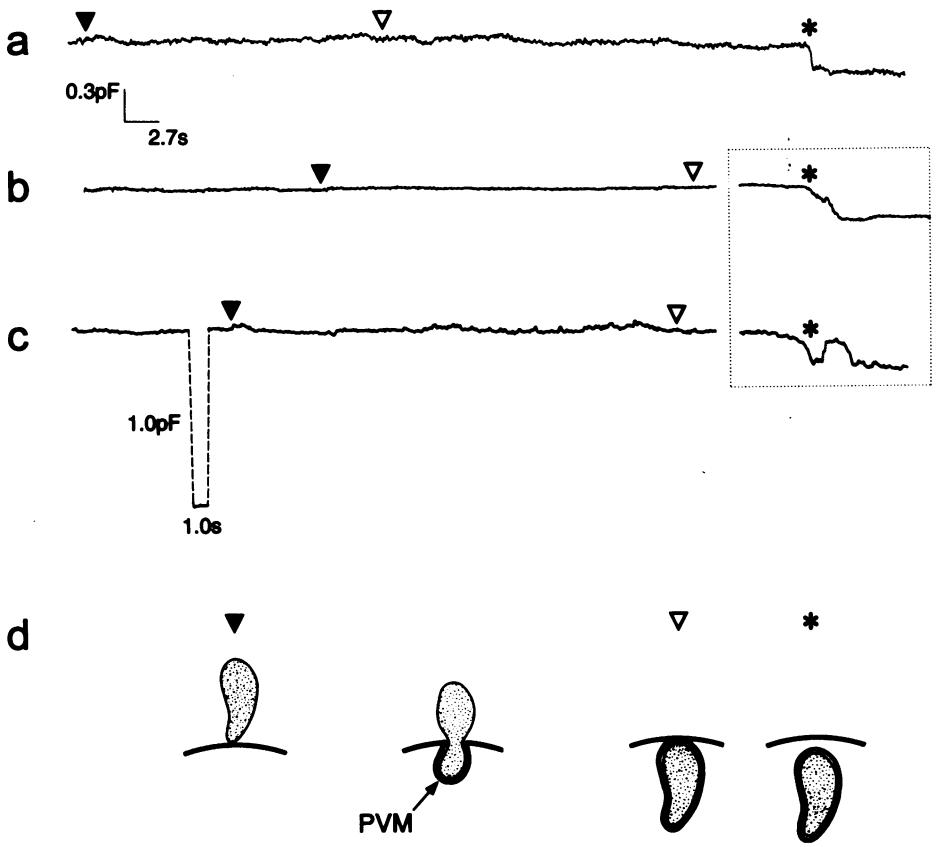

FIG. 2. (*a*) There is no significant change in host cell surface area during invasion. Three traces of cell capacitance during invasion are shown in *a–c*. Breaks were introduced into traces b and c (lined box) due to the total length of invasion in these cells (see below). The time of the spike is indicated in all traces by (▼), and the EOC by (▽). The model of PVM formation shown in *d* illustrates the approximate times at which the parasite in trace c is: attached (▼), finished constricting (▽)-the PVM is still continuous with host cell membrane, and internalized with the PVM pinched off (asterisk). The large downward step in trace c is an example of a 1 pF, 1 sec capacitance calibration mark. Pinching off of the PVM from the host cell is seen as a sudden drop in capacitance, occurring a variable time after EOC (34 sec, 279 sec, and 225 sec in *a*, *b*, and *c* respectively; asterisks).

modify the functional properties of the PVM. Our data are clearly inconsistent, however, with the idea that the PVM is composed primarily of lipids secreted by the parasite (11, 18, 31). They are also inconsistent with an earlier model in which the parasite enters directly into the host cell cytoplasm by disrupting a region of host plasma membrane (32), as this model would not predict the PVM-sized drops in host cell capacitance shown here (Fig. 2*a–c*). Studies of the PVM will now focus on questions of how the invagination is induced, and how a vacuole derived from the host cell membrane can resist fusion with the endolysosomal system of the host cell (4, 5).

We have demonstrated an unexpected delay between the EOC and the pinching off of the PVM. This delay occurred even under perforated patch conditions, which minimize cytoplasmic washout (23). Preliminary experiments using fluorescent antibody against the parasite surface protein P-30 and fluorescent lipophilic probes suggest that prior to pinching off, the PVM is continuous with the host plasma membrane but its interior is inaccessible to extracellular soluble macromolecules. This is reminiscent of the constricted pit stage of receptor-mediated endocytosis (33), and may represent a period of time during which host and/or parasite factors playing a role in the pinching off of the PVM can be studied. Host cell plasma membrane proteins that might normally target an endocytic vacuole for fusion with the endolysosomal system are apparently somehow removed from the *Toxoplasma* PVM shortly after parasite internalization (5). The lag period may provide the parasite with an opportunity to return these unwanted targeting signals to the host plasma membrane prior to pinching off of the PVM.

Pinching off of a vacuole from the plasma membrane involves the formation of a neck through the bending of the continuous, unitary membrane which comprises and links the plasma and vacuolar membranes, followed by severe constriction (to molecular dimensions) of this neck and a fission event during which the neck breaks and two distinct membranes emerge from the one. The parasitic fission pore observed during PVM pinch off was in many respects indistinguishable from the endocytic fission pore seen during membrane retrieval following exocytosis in the pituitary nerve terminal (25). Both demonstrated intermediate semistable conductance phases, and both showed a smooth, continuous decline in conductance prior to final closure. Compared with membrane fusion (34), membrane fission appears to be a slow process and is characterized by a continuous narrowing of a small pore with no final jump, while in membrane fusion, a distinct jump in pore conductance is observed prior to pore growth (27). The reversals in pore narrowing we have observed in the parasitic fission pore are occasionally seen in exocytotic fusion pores (34), but not as abruptly as seen here. Furthermore, we have seen no evidence of reopening of a completely closed parasitic fission pore (analogous to exocytotic flicker; ref. 35). It is tempting to regard the rapid re-enlargement of the almost-closed fission pore as a reflection of the disaggregation of, or escape from, a putative proteinaceous constricting apparatus around the cytoplasmic neck of the pore.

When the PVM cannot pinch off, invasion is arrested and the host cell lyses (36). Future studies of the parasitic fission pore may therefore yield new insights not only into the structure of the endocytic fission pore but also may help generate novel strategies to arrest infection.

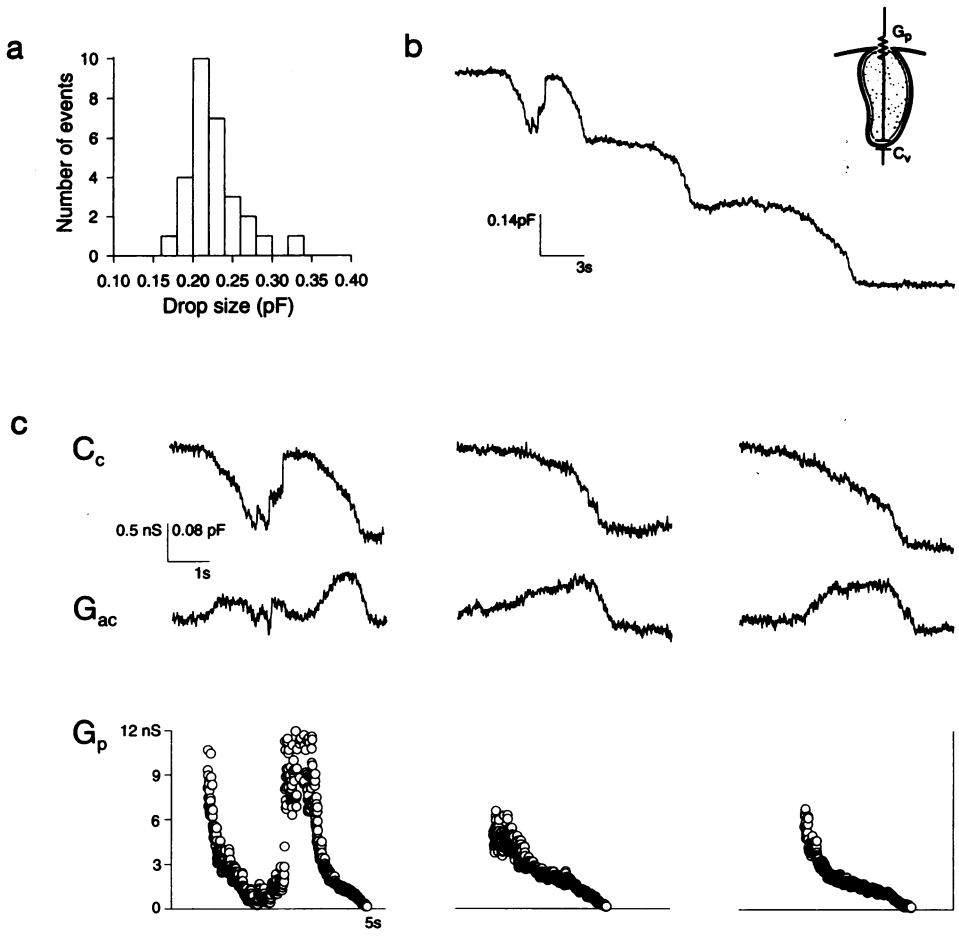

FIG. 3. (*a*) Histogram of the sizes of the capacitance drops associated with pinching off of the PVM. The mean size of the capacitance drop was 0.219 pF ± 0.006 pF (SEM, $n = 29$). (*b*) Multiple invasions into the same cell result in multiple drops in cell capacitance, all of similar size (0.22, 0.21, and 0.23 pF). The first capacitance drop in this series fluctuates once prior to pinching off completely. (*Inset*) Simplified equivalent circuit of parasite invasion used to calculate parasitic fission pore conductance (G_p). Cell and vacuolar conductance are neglected, and cell capacitance, vacuolar capacitance (C_v), and pipette access resistance are assumed to be constant constant during the relatively short time of fission pore measurement (20). (*c*) Fission pore conductances of the three capacitance drops shown in (*b*) were calculated from the out-of-phase and in-phase components of the measured admittance (C and G_{ac}).

We are grateful to Vladimir Ratinov for his generous assistance in many aspects of this work, and his programming of the digital lock-in. We thank Louis H. Miller for his support, and James Dvorak, Con Beckers, David Sibley, Paul S. Blank, and Jim Trimmer for helpful discussions.

1. Luft, B. J. & Remington, J. S. (1992) *Clin. Infect. Dis.* **15,** 211–220.
2. Kasper, L. H. & Boothroyd, J. C. (1993) in *Immunology and Molecular Biology of Parasitic Infections,* ed. Warren, K. S. (Blackwell, Boston), pp. 269–301.
3. Morisaki, J. H., Heuser, J. E. & Sibley, L. D. (1995) *J. Cell Sci.* **108,** 2457–2464.
4. Joiner, K. A. (1994) *Infect. Agents Dis.* **2,** 215–219.
5. Sibley, L. D., Dobrowolski, J., Morisaki, J. H. & Heuser, J. E. (1994) in *Strategies for Intracellular Survival of Microbes,* ed., Russell, D. G. (Bailliere Tindall, London), pp 245–264.
6. Elmendorf, H. G. & Haldar, K. (1993) *Parasitol. Today* **9,** 98–102.
7. Elford, B. C., Cowan, G. M. & Ferguson, D. J. P. (1995) *Biochem. J.* **308,** 361–374.
8. Ward, G. E., Miller, L. H. & Dvorak, J. A. (1993) *J. Cell Sci.* **106,** 237–248.
9. Ward, G. E., Chitnis, C. E. & Miller, L. H. (1994) in *Strategies for Intracellular Survival of Microbes,* ed., Russell, D. G. (Bailliere Tindall, London), pp. 155–190.
10. Mitchell, G. H. & Bannister, L. H. (1988) *CRC Crit. Rev. Oncol. Hematol.* **8,** 255–310.
11. Joiner, K. A. (1991) *Parasitol. Today* **7,** 226–227.
12. McLaren, D. J., Bannister, L. H., Trigg, P. I. & Butcher, G. A. (1979) *Parasitology* **79,** 125–139.
13. Aikawa, M., Miller, L. H., Rabbege, J. R. & Epstein, N. (1981) *J. Cell Biol.* **91,** 55–62.
14. Atkinson, C. T., Aikawa, M., Perry, G., Fujino, T., Bennett, V., Davidson, E. A. & Howard, R. J. (1987) *Eur. J. Cell Biol.* **45,** 192–199.
15. Dluzewski, A. R., Fryer, P. R., Griffiths, S., Wilson, R. J. M. & Gratzer, W. B. (1989) *J. Cell Sci.* **92,** 691–699.
16. Bannister, L. H., Mitchell, G. H., Butcher, G. A. & Dennis, E. D. (1986) *Parasitology* **92,** 291–303.
17. Stewart, M. J., Schulman, S. & Vanderberg, J. P. (1986) *Am. J. Trop. Med. Hyg.* **35,** 37–44.
18. Bannister, L. H. & Mitchell, G. H. (1989) *J. Protozool.* **36,** 362–367.
19. Neher, E. & Marty, A. (1982) *Proc. Natl. Acad. Sci. USA* **79,** 6712–6716.
20. Zimmerberg, J., Curran, M., Cohen, F. S. & Brodwick, M. (1987) *Proc. Nat. Acad. Sci. USA* **84,** 1585–1589.
21. Shi, G., Kleinklaus, A. K., Marrion, N. & Trimmer, J. S. (1994) *J. Biol. Chem.* **269,** 23204–23211.
22. Hamill, O. P., Marty, A., Neher, E., Sakmann, B. & Sigworth, F. J. (1981) *Pflugers Arch.* **391,** 85–100.
23. Horn, R. & Marty, A. (1988) *J. Gen. Physiol.* **92,** 145–159.
24. Cole, K. S. (1968) in *Membranes, Ions and Impulses* (Univ. of California Press, Berkeley).
25. Rosenboom, H. & Lindau, M. (1994) *Proc. Natl. Acad. Sci. USA* **91,** 5267–5271.
26. Niles, W. D., Levis, R. A. & Cohen, F. S. (1988) *Biophys. J.* **53,** 327–335.

27. Breckenridge, L. J. & Almers, W. (1987) *Nature (London)* **328,** 814–817.
28. Beckers, C. J. M., Dubremetz, J. F., Mercereau-Puijalon, O. & Joiner, K. A. (1994) *J. Cell Biol.* **127,** 947–961.
29. Sam-Yellowe, T. Y., Shio, H. & Perkins, M. E. (1988) *J. Cell Biol.* **106,** 1507–1513.
30. Mikkelsen, R. B., Kamber, M., Wadwa, K. S., Lin, P.-S. & Schmidt-Ullrich, R. (1988) *Proc Nat. Acad. Sci. USA* **85,** 5956–5960.
31. Dluzewski, A. R., Mitchell, G. H., Fryer, P. R., Griffiths, S., Wilson, R. J. M. & Gratzer, W. B. (1992) *J. Cell Sci.* **102,** 527–532.
32. Nichols, B. A. & O'Connor, G. R. (1981) *Lab. Invest.* **44,** 324–335.
33. Takei, K., McPherson, P. S., Schmid, S. L. & De Camilli, P. (1995) *Nature (London)* **374,**186–190.
34. Curran, M. J., Cohen, F. S., Chandler, D. E., Munson, P. J. & Zimmerberg, J. (1993) *J. Membr. Biol.* **133,** 61–75.
35. Fernandez, J. M., Neher, E. & Gomperts, B. D. (1984) *Nature (London)* **312,** 453–455.
36. Dvorak, J. A., Miller, L. H., Whitehouse, W. C. & Shiroishi, T. (1975) *Science* **187,** 748–750.